# Production of lignocellulose nanofibers from wheat straw by different fibrillation methods. Comparison of its viability in cardboard recycling process

Eduardo Espinosa,[a*] Fleur Rol,[b] Julien Bras,[b, c] Alejandro Rodríguez[a]

[a] Universidad de Córdoba, Departamento de Ingeniería Química, Campus de Rabanales, 14014 Córdoba, Spain

[b] Univ. Grenoble Alpes, CNRS, Grenoble INP, LGP2, F-38000 Grenoble, France

[c] Institut Universitaire de France (IUF), F-75000 Paris, France

* Corresponding author : eduardo.espinosa@uco.es

**7532 words**

**ORCID Number:**

Eduardo Espinosa: 0000-0002-5195-1557

Fleur Rol: 0000-0001-8353-3889

Julien Bras: 0000-0002-2023-5435

Alejandro Rodríguez: 0000-0001-8196-5848

## Abstract

The primary aim of this work was to evaluate various methods of nanocellulose production from wheat straw soda pulp. Wheat straw was cooked in 7 % NaOH (over dried material.) at a liquid/solid ratio of 10/1 at 100 °C for 150 min to obtain unbleached semichemical pulp. Lignocellulose nanofibers were produced by fibrillation in a high pressure homogenizer, ultrafine friction grinder or twin-screw extruder of cellulose fiber previously extracted from the pulp. Optimizing lignocellulose nanofibers production with the twin-screw extruder required using an enzymatic pretreatment. The three fibrillation methods were assessed for energy use and the resulting lignocellulose nanofibers were characterized in terms of morphology, crystallinity, thermal stability, chemical structure and mechanical properties. Adding lignocellulose nanofibers in proportions from 1.5 to 4.5 % to recycled cardboard pulp was found to considerably improve the mechanical properties of recycled fluting even in relation to pulp refining. Thus, the addition of

lignocellulose nanofibers doubled Young's modulus and burst index. The technical and energy feasibility of both processes was examined in order to evaluate the suitability of the different nanocellulose production methods for producing cardboard reinforcing agents as compared to conventional mechanical refining methods. This technology provides an economically more viable and competitive production process than industrial mechanical refining, presenting this technology as a candidate to improve the cardboard recycling process, at a lower cost, and increase the maximum recycling cycles that the product can support.

Keywords: Lignocellulose nanofibers (LCNFs), Mechanical nanofibrillation, Process energy efficiency, Recycled Cardboard, Mechanical Properties.

## 1. Introduction

Growing environmental concern has promoted an increasing use of natural resources. An estimated 1–3 × $10^{11}$ tons of cellulose, the most abundant polymer on earth, is produced by nature each year (Bovey and Winslow, 1981). This biopolymer is being increasingly used to develop novel bio-based efficient materials in order to alleviate the current global dependence on fossil fuels (Mohanty et al. 2002). The agricultural sector produces around 1.4 × $10^{11}$ tons of biomass every year a sizeable portion of which including leaves, roots, stalks, bark, bagasse, straw residues and seeds is dealt with as waste (Perlatti et al. 2014). By virtue of its abundance and very low cost, agroindustrial waste possesses a high chemical, material and energy potential (Lin and Luque, 2014; Tuck et al. 2012). Cereals account for 32 % of the global production of food products, with an annual figure of 2.85 × $10^{11}$ tons. Also, cereal production is expected to increase by as much as 15 % by 2023 in some countries, particularly in underdeveloped regions, in response to the increasing demand for food of a growing population (FAO, 2016; OECD/FAO, 2014). In the process, vast amounts of straw are being produced each year that are used mainly as feed for livestock or agricultural supplements when the lignocellulosic matrix of plant cell walls in these agricultural residues could be used as a source of cellulose or even nanocellulose (García et al. 2016).

The promising transparency, barrier and mechanical properties of nanosized cellulose fibrils as a bio-based, biodegradable, biocompatible nanomaterial have aroused increasing interest in them as building blocks for the development of new biomaterials (Liu et al. 2016). Nanocellulose is currently being used as an ingredient of food packaging (Azeredo et al. 2012) and conductive materials (Du et al. 2017; Hoeng et al. 2017), for purposes such as bioremediation of wastewater and $CO_2$ capture (Putro et al. 2017; Venturi et al. 2018) and the development of analytical sensors (Ruiz-Palomero et al. 2017) and medical devices (Lin and Dufresne, 2014) or even as a food additive (Corral et al. 2017). The characteristics of nanocellulose depend on the chemical and physical properties of the fibers from which it is made, whether the fibers are treated mechanically or chemically, and the mechanical method used for nanofibrillation (Nechyporchuk et al.

2016; Rol et al. 2019). Bleached cellulose pulp provides “cellulose nanofibers” (CNFs) and unbleached pulp gives “lignocellulose nanofibers” (LCNFs).

Pulp fibers can be nanofibrillated mechanically by using an ultra-fine grinder, a high-shear homogenizer or a microfluidizer. The process is facilitated by various pretreatments that weaken cellulose fibers and reduce energy consumption as a result. The pretreatments influence the morphological, mechanical and surface properties of the resulting material (Dufresne, 2013). The most widely used chemical pretreatments include TEMPO-mediated oxidation, enzymatic prehydrolysis and cationization of cellulose fibers. Nanofibrillation uses a large amount of energy, which is a serious hindrance to CNF production at an industrial scale. Also, classical mechanical treatments provide low nanocellulose yields (< 5 %), which increases raw material transportation and storage costs, and restricts some applications such as painting (Rol et al. 2017). In recent years, the twin-screw extruder (TSE) has proved an effective alternative for nanocellulose production as it provides high CNF yields (20–30 %) with less energy consumption than the conventional processes (Baati et al. 2017; Ho et al. 2015; Rol et al. 2017).

Hornification during the drying stage in the paper production process causes the internal fiber volume to shrink. As a result, hornified recycled paper has poor hydration and swelling related properties such as tensile strength or burst index (Minor, 1994). Mechanical refining of recycled paper can restore the swelling capacity of hornified fibers by increasing their fines content and surface area, thereby facilitating fiber–fiber bonding; after a number of cycles, however, the adverse effects of hornification cannot be reversed.

Cellulose nanofibers have gained increasing attention as coatings or dry and wet strength agents for papermaking (Bardet and Bras, 2013; Eriksen et al. 2008) and also in engineering constructions (Zhang et al. 2018). The growing use of CNFs by the papermaking industry can be ascribed mainly to the following facts: (*a*) their nanometric width, which increases their surface area; (*b*) their micrometric length; (*c*) their high intrinsic mechanical strength and good flexibility; (*d*) their high potential for hydrogen

bonding to cellulose fibers; and (*e*) their ability to form strong entangled networks (Boufi et al. 2016).

Nanocellulose can reduce structural damage caused by mechanical refining and increase the number of cycles over which paper can be reused as a result. Recent advances in pretreatments and fibrillation processes have reduced energy consumption in CNF production, thereby opening up new avenues for technically and economically viable paper and cardboard recycling. However, most advances in this direction are fairly recent and few studies have to date focused on them in connection with wood based nanocellulose.

In this work, semichemical soda pulp from wheat straw was used to obtain different lignocellulosic nanofibers (LCNFs). In this work, LCNFs were obtained by mechanical processing with a twin-screw extruder (TSE), a high pressure homogenizer (HPH) or an ultra-fine grinder (UFG). Also, an enzymatic hydrolysis pretreatment was used to improve nanofibrillation with the TSE. The LCNF samples thus obtained were characterized and added to recycled pulp cardboard to assess their reinforcing capacity. The mechanical refining method typically used to reinforce recycled pulp cardboard and the addition of LCNF were compared in terms of energy consumption in order to evaluate the feasibility of the proposed technology. To the best of our knowledge, no energy viable method of producing nanocellulose had been described before in comparison with the conventional mechanical refining for the cardboard recycling process. This finding opens the door to adopt this technology in industry and improve recycling processes, in turn increasing the number of recycling cycles that the cardboard can withstand.

## 2. Materials and methods

***2.1. Materials.*** The raw material used was wheat straw with a moisture content of (8.00 ± 0.31) % that was screened by hand to remove undesired elements. The chemicals used included acetic acid ($CH_3COOH$, ACS reagent, ≥ 99.7 %), acetone ($C_3H_6O$), hydrochloric acid (HCl), FiberCare® (Novozymes, Copenhagen, Denmark), sodium bromide (NaBr, BioUltra, ≥ 99.5 %), sodium acetate trihydrate ($NaCH_3COO \cdot 3H_2O$, ReagentPlus, ≥ 99.0

%), sodium chloride (NaCl, > 99 %), sodium hydroxide (NaOH) and sodium chlorite ($NaClO_2$, Sigma–Aldrich, technical grade 80 %), and were all used as received.

***2.2. Production of Cellulose Pulp.*** Wheat straw was subjected to soda pulping at 100 °C, for 150 min, using 7 % soda over dried material (o.d.m.) at a liquid/solid ratio of 10/1 in a 15 L batch reactor heated by an outer jacket heater and stirred by rotating the reaction vessel with a motor. 500 grams of dry wheat straw are added to the reactor. Then, 7% (calculated on 500 grams) of a solution of sodium hydroxide is added and completed with water until the fixed liquid/solid ratio is reached. After the pulping process, the cellulosic pulp is washed to remove the reagent and soluble substances, and then passed through a Sprout Bauer, thus obtaining a semi-chemical pulp.The resulting cellulose pulp was characterized for beating (Tappi T248), yield (gravimetric method), α-cellulose (Tappi T203), lignin (Tappi T222), holocellulose (Tappi T212), ash (Tappi T244), ethanol extractives (Tappi T204), kappa number (Tappi T236) and viscosity (Tappi T230).

***2.3. Mechanical Pretreatment.*** Cellulose fibers were suspended in a proportion of 10 % in water and refined to a Schopper–Riegler degree of 90 (ISO 5267-1) on a PFI Beater from Metrotec (Kirchheim, Germany). All measurements were made at least in triplicate.

***2.4. Enzymatic Pretreatment.*** An aqueous suspension, containing 2 wt% cellulose fiber, was hydrolyzed by using a FiberCare® endoglucanase solution. pH was adjusted to 5 with a buffer consisting of sodium acetate trihydrate and acetic acid. Then, the suspension was supplied with a 300 ECU/g concentration of enzymes, and allowed to react at 50 °C for 2 h. After that, the reaction was stopped by heating at 90 °C for 15 min to denature the enzymes. The suspension was then filtered and washed with deionized water.

***2.5. Production of Lignocellulose Nanofibers.*** Once pretreated, cellulose fibers were subjected to three different treatments to obtain LCNFs as follows:

I. A suspension, containing 2 wt% cellulose fiber, was fibrillated at 2500 rpm for 2.5 h on a Supermasscolloider ultra-fine friction grinder (Model MKZA6-2, disk model MKG-C 80, Masuko Sangyo Co., Ltd., Kawaguchi, Japan) equipped with recirculation. The maximum gap between the two disks was –10. The pulp was passed for 1 s approximately 60 times per hour through the nip zone.

II. A cellulose fiber suspension, with a high solid content (18–20 wt%), was passed through a twin-screw extruder (Thermoscientific HAAKE Rheomex OS PTW 16 + HAAKE PolyLab OS RheoDrive 7, L/D ratio = 40). The TSE screws were a combination of kneading disks and fully flighted conveying screws. The temperature was kept at ca. 10 °C by recirculating water, and the apparatus was operated at 400 rpm. The screw profile used was similar to that reported by Rol et al. (2017).

III. A 1.5 wt% fiber suspension was passed through a high pressure homogenizer (PANDA GEA 2 K NIRO) four times at 300 bar, three at 600 bar and three at 900 bar.

***2.6. Characterization of Lignocellulose Nanofibers.*** LCNF samples were characterized in terms of nanofibrillation yield, optical transmittance, carboxyl content, cationic demand and degree of polymerization, and by thermogravimetric analysis and X-ray diffraction spectroscopy.

Nanofibrillation yield was determined by centrifuging a 0.1 wt% fiber suspension at 10000 rpm for 12 min to isolate nanofibrillated material from nonfibrillated, or partially fibrillated material, according to Besbest et al. (2011) The optical transmittance of a 0.1% LCNF suspension, used as an indirect indicator of nanofibrillation yield, was measured in the region 400–800 nm on a Lambda 25 UV spectrometer from Perkin Elmer (Waltham, MA, USA). The carboxyl content (CC) of the LCNFs was determined by conductometric titration as described elsewhere (Besbes et al., 2011). Thus, CC was calculated from the volume of a 0.01 N NaOH solution required to neutralize weak acid groups (carboxyl groups) in the fibers. The cationic demand (CD) of the fibers was

determined by using a Mütek PCD 05 particle charge detector according to Espinosa et al. (2017). The specific surface area of the LCNFs and their theoretical diameter were calculated from the stoichiometric relationship between hydroxyl and carboxyl groups with poly-DADMAC surface adsorption on the fibers (Espinosa et al., 2016). The intrinsic viscosity ($\eta_s$) of each sample was calculated from its degree of polymerization, which was determined according to ISO 5351:2010. Each sample was measured 5 times to calculate and average value and its standard deviation. The degree of polymerization (DP) was calculated from eq. 1 when it was lower than 950 or eq. 2 otherwise (Marx-Figini, 1987):

$$DP = (\eta_s/0.42) \quad (1)$$

$$DP^{0.76} = (\eta_s/2.28) \quad (2)$$

Thermogravimetric analyses (TGA) were performed on a Mettler Toledo TGA/DSC 1 instrument. Thermal stability was assessed by heating samples from room temperature to 800 °C at a rate of 10 °C/min, using a nitrogen stream at a flow rate of 50 mL/min. The TGA equivalent derivative (DTG) was calculated to determine the temperature at the maximum degradation rate ($T_{max}$).

X-ray diffraction (XRD) patterns were obtained on a Bruker D8 Discover spectrometer equipped with a CuKα1 monochromatic source. Patterns were recorded over the 2θ range 7–50°, using a scan speed of 1.56 °/min. The Crystallinity Index (CI) was calculated by using the method of Segal (Segal et al. 1959), which is based on the intensity of the (200) peak ($I_{200}$) and the minimum distance ($I_{am}$) between the peaks for planes (200) and (110):

$$CI = \frac{I_{200} - I_{am}}{I_{200}} \cdot 100 \quad (3)$$

***2.7. Calculation of the Energy Demand.*** The energy demand of the homogenizer and ultra-fine grinder was calculated as that required by the electrical grid of the equipment. The specific mechanical energy (SME), in kWh/t, used by the TSE was calculated from the following equation (Domenech et al. 2013; Gogoi et al. 1996; Liang et al. 2002):

$$SME = \frac{N*C*Q}{N_{max}*P_{max}*C_{max}} \quad (4)$$

Where $N$ is the rotational speed (rpm), $N_{max}$ its maximum value (1100 rpm), $P_{max}$ the maximum pressure (7 kW), $C$ (N·m) the torque as measured on the extruder motor, $C_{max}$ the maximum torque (130 N·m) and $Q$ the dry flow rate (t/h).

***2.8. Reinforcement of recycled cardboard.*** Addition of LCNFs in a proportion of 1.5%, 3% or 4.5% and mechanical refining for 1000, 2000 or 3000 revolutions were used to improve the mechanical properties of recycled cardboard. For this purpose, an LCNF suspension was dispersed in recycled cardboard slurry by using a pulp disintegrator at 1.5 % consistency at 3000 rpm for 60 min. Due to the need to use retention agents to retain LCNF on the fiber and not lose them in the cardboard forming process, cationic starch and colloidal silica in a proportion of 0.5 and 0.8 %, respectively, were incorporated into the pulp slurry under gentle stirring for 20 min. (Delgado-Aguilar et al. 2015; Tarrés et al. 2016). The use of these retention system can promote the occurrence of fiber flocs thus affecting the uniformity of the sheet and therefore the performance of paper. To avoid this problem colloidal silica is used as deflocculant to prevent floc formation and avoid problems during sheet formation. The negatively charged particles of colloidal silica have a great interaction with the positive surfaces of the fibers, once the cationic starch is added and retain on the fibers, and this interaction avoid the fibers flocs formation, making the distribution of fiber in the sheet much better. Sheets with a basis weight of 60 g/m$^2$ were prepared according to ISO 5269-2 on an ENJO-F-39.71 former and conditioned in a weather chamber at 23 °C at 50 % relative humidity for 48 h before mechanical testing. Once conditioned, sheets were analyzed for breaking length and Young's modulus at a constant elongation rate, according to ISO 1942-2, using an LF Plus testing machine from Lloyd Instruments (Bognor Regis, UK) equipped with a 1 kN load cell. Tear index was determined according to ISO 1974 on an Elmendorf Tearing Tester (mod. F53.98401 Frank PTI). Finally, burst index was determined according to ISO 2758 on a burst tester (IDM mod. EM-50). The physical properties of the sheets were analyzed for their

thickness, density, Gurley porosity and porosity. The thickness was determined according to the standard ISO 534. The density was calculated from the weight of the sheets and their dimensions. The Gurley porosity was determined using a Gurley porosimeter (Papelquimia) according to ISO standard 5636/5. The porosity of the sheets was calculated using the next equation:

$$Porosity\ (\%) = 100 \cdot \left(1 - \frac{\rho_{sample}}{\rho_{cellulose}}\right) \quad (5)$$

where $\rho_{sample}$ is the density of the sheet, and $\rho_{cellulose}$ is the density of cellulose, assumed as 1.5 g/cm$^3$.

The topography and roughness of the surface of the sheets were analyzed by 3D reconstructions by Zeta3D Optical Profiler model Zeta-20 (Zeta Instruments). The surface of the sheets and the interaction LCNF-fiber was also studied by scanning electron microscopy (SEM). The microscope was a JEOL JSM 6300 – SEM – EDX and images were acquired at 100x and 1000x, in secondary electron imaging mode. The acceleration voltage and working distance were 5 kV and 10 mm, respectively.

## 3. Results and discussion

As determined in previous work, the wheat straw used as raw material contained α-cellulose (39.7 %), hemicelluloses (30.6 %), lignin (17.7 %) and other, nonstructural elements including alcohol extractives (5.2 %) and ash (7.7 %) (Espinosa et al. 2017). Soda pulping of the straw provided cellulose pulp with an increased α-cellulose content (62 %), and decreased hemicellulose, lignin, extractives and ash contents (23.3 %, 9 %, 1.65 % and 1.52 %, respectively).

### *3.1. Nanocellulose from wheat straw*

Lignocellulose nanofibers were obtained by subjecting cellulose pulp fibers to three different treatments. The different treatments differ in the mechanism and way of producing the mechanical forces to the fiber for its nanofibrillation. In the HPH, the cellulose fiber suspension is pumped at high pressure through a small gap present in the

265 homogenizer chamber created by an impact ring and a valve which is opened and closed
266 rapidly to submit to the fibers to high shear and impact forces, producing the
267 nanofibrillation. During the treatment of UFG, the cellulose suspension is passed through
268 a rotary and static stones separated by a variable distance which is decreased with the
269 number of passes. The passage through both discs produces high shear forces and the
270 cellulose fiber are delaminated. In the TSE, a cellulose suspension at high solid content
271 (20 – 40%) passed through a co-rotative twin screw extruder where friction forces are
272 produced between the screws and produce the reduction in fiber size (Rol et al. 2019). A
273 schematic view of the different treatments used in this work is shown in the **Figure S1**.
274 The treatments with the HPH, UFG and TSE were preceded by mechanical refining of
275 the pulp to a Schopper–Riegler degree of 90 to facilitate subsequent nanofibrillation, Enz-
276 TSE had an enzymatic pretreatment prior to refine process as mechanical treatment.
277 The suitability of the nanofibrillation treatments was evaluated in terms of the
278 characteristics of the resulting lignocellulose nanofibers, which are summarized in **Table**
279 **1**.
280 Based on nanofibrillation yields, the nanofibers provided by the HPH contained
281 more nanofibrillated material than did those obtained with UFG and, especially, TSE.
282 However, the enzymatic pretreatment increased the nanofibrillation yield of the TSF from
283 15.17 % to 42.31 %, which exceeded the UFG value. This result testifies to the efficiency
284 of the new TSE-based mechanical process in combination with an enzyme pretreatment.
285 The transmittance values of the LCNF films, which are used as indirect indicators
286 of nanofibrillation yield, followed the same sequence as the yields. Because cationic
287 demand (CD) represents the ability of nanofiber surfaces to interact with their
288 environment (fibers, fines, water) during cardboard production, a high CD value is
289 desirable to ensure effective binding of nanofibers as a cardboard reinforcement. As
290 expected, and consistent with the nanofibrillation yields, the HPH and Enz–TSE
291 treatments led to the greatest CD values.
292 The carboxyl contents of the different LCNFs were similar to those for other
293 materials obtained with enzymatic and mechanical treatments (Delgado-Aguilar et al.

2016; Espinosa et al. 2017; Vallejos et al. 2016) but lower than those of CNFs obtained by TEMPO-mediated oxidation (ca. 1200 μeq·g/g) (Besbes et al. 2011; Puangsin et al. 2013; Saito et al. 2005). The specific surface area and diameter of individual lignocellulose nanofibers were estimated from their CD values and carboxyl contents as described elsewhere (Espinosa et al. 2016) and successfully done in previous studies (Delgado-Aguilar et al. 2016; Espinosa et al. 2017). Nanofiber diameters (13–22 nm) and lengths (0.9–5 μm) were similar among samples. The nanometric size of the LCNFs was confirmed by AFM (**Figure S2**). All mechanical treatments provided LCNFs longer than 4 μm but those obtained with an enzymatic pretreatment were only 0.9 μm long owing to the shearing action of the endoglucanases used. For this reason, the Enz–TSE treatment led to the lowest L/D (aspect) ratio and the HPH treatment to the highest.

The chemical structure of the LCNFs was examined by FTIR spectroscopy. As can be seen from **Figure S3**, all samples exhibited the typical spectra for lignocellulosic materials including bands for stretching vibrations of –OH and –CH groups in the cellulose structure at 3300 and 2900 $cm^{-1}$. The band at 1604 $cm^{-1}$ was assigned to C=O stretching of carboxyl groups and that at 1515 $cm^{-1}$ to stretching of C=C bonds in aromatic rings of lignin. No differences in chemical structure among samples were observed.

### *3.2. Influence of the mechanical treatment on nanofiber properties*

The degree of polymerization (DP) of cellulose is related to the length of its chains and provides information about the extent of cleavage along the fiber direction (Ho et al. 2015). As can be seen from **Figure 1**, DP was decreased by the mechanical treatments and enzymatic pretreatment. The initial DP value for cellulose fiber in wheat straw is 1469, and the mechanical treatments and enzymatic pretreatment decreased it by 4.15 and 60.50 %, respectively. Each pass through the extruder reduced DP by about 72.23 and 17.5 % with and without an enzymatic pretreatment, respectively. The substantial decrease in DP caused by the enzymatic pretreatment was a result of the enzymes attacking amorphous domains in cellulose as reported elsewhere (Henriksson et al. 2007;

323 Rol et al. 2017). The HPH and UFG decreased DP by 9.5 and 21.85 %, respectively, as
324 compared to about 30% reported by Henriksson et al. (2007) and Iwamoto et al. (2007).
325 The influence of the mechanical treatments and enzymatic pretreatment on
326 crystallinity was examined by X-ray diffraction analysis. **Figure 2** shows the X-ray
327 diffraction patterns for the different types of LCNFs. The patterns contained the typical
328 peaks for Cellulose I at 2θ values of 15° and 23°, corresponding to the (101) and (002)
329 plane, respectively. Cellulose pulp from wheat straw has a crystallinity index of 57.20 %
330 that was decreased by the mechanical treatments through collapse of the crystalline
331 domains in cellulose. The HPH and UFG treatments decreased crystallinity to a much
332 smaller extent than the TSE treatment (1.5–2 vs 7 %, the latter value being similar to the
333 losses observed in other studies) (Ho et al. 2015; Rol et al. 2017). However, the LCNFs
334 obtained with TSE in combination with the enzymatic pretreatment exhibited increased
335 crystallinity as a result of the sheering effect of endoglucanase on the amorphous part of
336 cellulose leading to shorter, more crystalline fibers (Espinosa et al. 2017; Nechyporchuk
337 et al. 2015). These results, however, should be accepted with caution since the assessment
338 method was developed for pure cellulose rather than lignocellulosic samples and CI is
339 representative of crystal quality but not of the proportion of crystalline and amorphous
340 components.
341 The potential of the LCNFs for use in high-temperature applications such as
342 papermaking, composite production or plastic reinforcement was evaluated by assessing
343 their thermal stability. **Figure 3** shows the thermogravimetric (TG) curves and their
344 derivatives (DTG) for the LCNFs. All the samples exhibited an initial weight loss
345 corresponding to moisture. The main loss feels in the range of 300–400 °C and was due
346 to thermal degradation of cellulose. Based on the results, there were no significant
347 differences in thermal stability between the LCNFs obtained with the UFG and TSE
348 treatments; by contrast, the nanofibers obtained with the HPH had a lower $T_{max}$ value by
349 effect of their greater specific surface area resulting in a higher surface area being exposed
350 to heat and thermal degradation as a result.
351

### *3.3. Use of lignocellulose nanofibers for reinforcing recycled cardboard*

Hornification weakens fibers and decreases their ability to bond to one another during the recycling of paper and cardboard, thereby causing a loss of mechanical properties (Minor, 1994). The simplest, most widely used industrial technology to reverse this loss is mechanical refining to increase the specific surface area of fibers in order to facilitate bonding to other fibers. However, this process also results in internal fibrillation and structural damage by effect of shearing during mechanical refining, which restricts the number of cycles over which cardboard can be recycled in practice (Delgado-Aguilar et al. 2015). Adding nanocellulose as a reinforcing agent to a pulp suspension during recycling allows that number of cycles to be increased from typically 3 to 10 or more (Delgado-Aguilar et al. 2015). In any case, obtaining nanocellulose with mechanical means such as a high pressure homogenizer or an ultrafine grinder requires more energy than conventional mechanical refining. New technologies such as twin screw extrusion, however, use less energy to produce nanocellulose and may thus be viable choices for cardboard recycling.

The industrial cardboard used here had a breaking length (BL) in the machine direction of 5656 m. Because that sheets used were obtained in an isotropic former, the target BL for improved recycled cardboard at an anisotropic ratio of 1.65 was 3443 m (Espinosa et al., 2018). **Figure 4** shows the variation of the mechanical properties of recycled cardboard samples resulting from the addition of LCNFs as compared with mechanical refining (PFI beating). The reinforcing effect of nanocellulose likely resulted from (*a*) the polymer favoring adhesion and bridging adjacent fibers, thereby facilitating interfiber bonding; or (*b*) its generating a different network embedded between larger fibers, thereby increasing the load bearing capacity of the substrate (Boufi et al. 2016). The breaking length, Young's modulus, burst index and tear index of the recycled cardboard were 2097 m, 1.15 GPa, 1.07 KPa·m$^2$/g and 5.55 mN·m$^2$/g, respectively. The mechanical properties of the cardboard increased similarly with increasing amount of LCNFs added and increasing strength of mechanical refining. In most samples, the target breaking length, 3443 m, was obtained with 1000 rev of mechanical refining or the

addition of LCNFs in a proportion of 1.5 %. Also, refining for 3000 rev and addition of a proportion of LNFCs of 4.5 % both increased BL up to about 4000 m. As a result, the mechanical properties increased in parallel with the degree of mechanical refining or amount of LCNFs added to the slurry. The increase was up to 100 % for breaking length (from 2000 to 4000 m), Young's modulus (1 to 2 GPa) and burst index (1 to 2 KPa·$m^2$/g), and about 30% for tear index (5.5 to 7.5 mN·$m^2$/g). The reinforcing effect obtained with mechanical refining and LCNFs was similar. However, it differed among refining techniques, the HPH and UFG having a stronger effect than the TSE. Also, there were no differences between the TSE samples obtained with and without an enzymatic pretreatment —by exception tear index was more markedly increased with the pretreatment (Enz–TSE).

In order to further study the effect of LCNF and mechanical refining on recycled cardboard, the evolution of physical properties was analyzed as shown in **Table 2**. The results indicate that cardboard thickness decreases with increasing LCNF content and mechanical refining intensity. This reduction can be explained by the free movement of the LCNF in the fiber suspension (in the same way that the fines behave), reducing the radius of the meniscus that appears during the dewatering of the suspension in the cardboard manufacture; this increases the pressure difference between the aqueous phase and the fiber surroundings, allowing to bring fibers close together, producing their compaction (Espinosa et al. 2016). This phenomenon also explains the increase in density compared to unreinforced recycled cardboard. Porosity, defined as the percentage of empty space in the structure formed by the fibers in the cardboard, also decreases as a result of the compaction. The same effect is observed when analyzing the Gurley porosity, which expresses the resistance (in seconds) exerted by the cardboard to the passage of a 100 mL air flow and is directly related to porosity and density. The decrease in thickness and porosity, and the increase in density and Gurley porosity, is more evident when using LCNF as reinforcing agent, especially those obtained by HPH and UFG, compared to mechanical refining. It is produced by the effect of the LCNF occupying the spaces

between the larger fibers, forming a nanometer network that occupies the gaps between the fibers, helping to reduce the diameter and number of pores in the cardboard.

The topography and roughness of the sheets was analyzed by profilometry (Figure S4). The results show how LCNF application and mechanical refining produce sheets with a smoother surface than those presented by unreinforced cardboard. This is due to the delamination of the fibers during the refining process, as well as the formation of a LCNF layer on the surface of the paper during its formation. This fact is also observed when analyzing the surface of the sheets by SEM (**Figure 5**). In addition, the effect of LCNF on fiber-fiber interaction (1000 magnifications) was observed, resulting in increased bonding capacity between fibers, as well as the occupation of free voids. This supports the explanation of the effect of LCNF on the physical and mechanical properties of the recycled cardboard.

**Figure 6** shows the variation of the drainage properties of recycled cardboard slurries containing different amounts of LCNFs and mechanically refined to a variable degree. As expected, such properties declined with increasing LCNF content and refining intensity of the slurry. This was a result of the increased specific surface area of the LCNFs resulting in a higher charge density and hence in more extensive binding of water to the fibers —and of refining increasing capillary forces and the water holding capacity of OH groups. Adding LCNFs to the slurries decreased drainage more markedly than did mechanical refining as a result of the nanofibers increasing the specific surface area and promoting hydrogen bonding with water. The increased surface area and charge density with the LCNFs led to an increased degree of refining (°SR), the effect increasing in the following treatment sequence: HPH > UFG > TSE > Enz-TSE. In any case, this adverse effect on drainage properties can be circumvented by using an appropriate combination of nanofibers and a polyelectrolyte (Eriksen et al. 2008).

### *3.4. Energy consumption for nanocellulose production*

One of the main drawbacks of the industrial production of cellulose nanofibers scale is the large amounts of energy it requires even if a mechanical refining, enzymatic

hydrolysis or TEMPO-mediated oxidation treatment is used to facilitate disintegration of fibers. The amount of energy used by the most common procedures for this purpose is about 30 000 kWh/t with a high pressure homogenizer (HPH) and 50 000 kWh/t with an ultrafine grinder (UFG), both on a dry weight basis, and greatly restricts their scope. By contrast, a twin-screw extruder (TSE) uses only about 4000 kWh/t (Baati et al. 2017; Chaker et al. 2015; Rol et al. 2017; Spence et al. 2011). The specific amounts of energy needed to obtain LCNFs with the HPH, UFG and TSE here are shown in **Figure 7**. Such amounts are similar to previously reported values (viz., 32 000, 30 000 and 6000 kWh/t for HPH, UFG and TSE, respectively). Also, as found in previous studies, using an enzymatic pretreatment in combination with the TSE reduced energy consumption by 37 % (Rol et al. 2017).

### *3.5. Energy consumption for recycling*

The viability of each technology for reinforcing recycled cardboard was evaluated from the amount of energy required for LCNF production and mechanical refining. As can be seen from **Figure 8**, if the effect on physical properties is assumed to be similar, then the HPH and UFG required 59 and 49 % more energy, respectively, than did conventional mechanical refining to have the same reinforcing effect. By contrast, the TSE reduced the amount of energy needed for recycling by 233 % in the absence of an enzymatic pretreatment and by 426 % in its presence. Therefore, using LCNFs obtained with a TSE is energy feasible for reinforcing recycled cardboard whether or not it is combined with an enzymatic pretreatment.

## Conclusions

The effect of the LCNFs on cardboard properties was comparable to that of conventional mechanical refining and the target properties were obtained by adding as low a proportion of LCNFs as 1.5 % to recycled cardboard. The Twin-screw extruder technology for lignocellulose nanofibers production required 5 times less energy than the high pressure homogenization and ultrafine grinder to produce nanocellulose —10 times

less if used jointly with an enzymatic pretreatment—, thus providing an advantageous alternative to both methods and even to conventional refining. A detailed study of the microstructure in paper formation will be carried out in the future to better understand the quality of the product obtained and to analyse the increase in the number of effective cycled of cardboard recycling that this technology allows. This work advances in the use of cellulose nanofibers in the cardboard recycling industry and provides an energy viable production method compared to the mechanical refining currently used. This technology corrects the deterioration in the physical properties of the cardboard produced by the hornification process, without physically modifying the fiber, thus allowing a greater number of cardboard recycling cycles, extending the useful life of the product and improving the sustainability of the process. This will be reflected in lower energy consumption and less incorporation of virgin fiber in the process.

## Acknowledgments

The authors are grateful to Spain's DGICyT, MICINN for funding this research within the framework of the Projects CTQ2016-78729-R and supported by the Spanish Ministry of Science and Education through the National Program FPU (Grant Number FPU14/02278), and also to the staff of the Central Service for Research Support (SCAI) at the University of Córdoba.

## References

Azeredo, H. M. C., Rosa, M. F., Mattoso, L. H. C., 2017. Nanocellulose in bio-based food packaging applications. Ind. Crop. Prod. 97, 664-671.

Baati, R., Magnin, A., Boufi, S., 2017. High Solid Content Production of Nanofibrillar Cellulose via Continuous Extrusion. ACS Sustain. Chem. Eng. 5(3), 2350-2359.

Bardet, R., Bras, J., 2013. *Cellulose Nanofibers and Their Use in Paper Industry*, in: *Handbook of Green Materials*, pp. 207-232.

Besbes, I., Alila, S., Boufi, S., 2011. Nanofibrillated cellulose from TEMPO-oxidized eucalyptus fibres: Effect of the carboxyl content. Carbohyd. Polym. 84(3), 975-983.

Boufi, S., González, I., Delgado-Aguilar, M., Tarrès, Q., Pèlach, M. À., Mutjé, P., 2016. Nanofibrillated cellulose as an additive in papermaking process: A review. Carbohyd. Polym. 154, 151-166.

Bovey, F. A., Winslow, E. H., 1981. *An Introduction to Polymer Science*. New York: Academic Press.

Chaker, A., Mutjé, P., Vilar, M. R., Boufi, S., 2014. Agriculture crop residues as a source for the production of nanofibrillated cellulose with low energy demand. Cellulose. 21(6), 4247-4259.

Corral, M. L., Cerrutti, P., Vázquez, A., Califano, A., 2017. Bacterial nanocellulose as a potential additive for wheat bread. Food Hydrocolloid. 67, 189-196.

Delgado-Aguilar, M., Gonzalez, I., Pelach, M. A., De La Fuente, E., Negro, C., Mutje, P., 2015. Improvement of deinked old newspaper/old magazine pulp suspensions by means of nanofibrillated cellulose addition. Cellulose. 22(1), 789-802.

Delgado-Aguilar, M., Gonzalez, I., Tarres, Q., Pelach, M. A., Alcala, M., Mutje, P., 2016. The key role of lignin in the production of low-cost lignocellulosic nanofibres for papermaking applications. Ind. Crop. Prod. 86, 295-300.

Delgado-Aguilar, M., Tarrés, Q., Pèlach, M. À., Mutjé, P., Fullana-i-Palmer, P., 2015. Are Cellulose Nanofibers a Solution for a More Circular Economy of Paper Products? Environ. Sci. Technol. 49(20), 12206-12213.

Domenech, T., Peuvrel-Disdier, E., Vergnes, B., 2013. The importance of specific mechanical energy during twin screw extrusion of organoclay based polypropylene nanocomposites. Compos. Sci. Technol. 75, 7-14.

Du, X., Zhang, Z., Liu, W., Deng, Y., 2017. Nanocellulose-based conductive materials and their emerging applications in energy devices - A review. Nano Energy. 35, 299-320.

Dufresne, A., 2013. Nanocellulose: a new ageless bionanomaterial. Mater. Today. 16(6), 220-227.

Eriksen, Ø., Syverud, K., Gregersen, Ø., 2008. The use of microfibrillated cellulose produced from kraft pulp as strength enhancer in TMP paper. Nord. Pulp. Pap. Res. J. 23, 299-304.

Espinosa, E., Dominguez-Robles, J., Sanchez, R., Tarres, Q., Rodriguez, A., 2017. The effect of pre-treatment on the production of lignocellulosic nanofibers and their application as a reinforcing agent in paper. Cellulose. 24(6), 2605-2618.

Espinosa, E., Sánchez, R., González, Z., Domínguez-Robles, J., Ferrari, B., Rodríguez, A., 2017. Rapidly growing vegetables as new sources for lignocellulose nanofibre isolation: Physicochemical, thermal and rheological characterisation. Carbohyd. Polym. 175, 27-37.

Espinosa, E., Sánchez, R., Otero, R., Domínguez-Robles, J., Rodríguez, A., 2017. A comparative study of the suitability of different cereal straws for lignocellulose nanofibers isolation. Int. J. Biol. Macromol. 103, 990-999.

Espinosa, E., Tarres, Q., Delgado-Aguilar, M., Gonzalez, I., Mutje, P., Rodriguez, A., 2016. Suitability of wheat straw semichemical pulp for the fabrication of lignocellulosic nanofibres and their application to papermaking slurries. Cellulose. 23(1), 837-852.

Espinosa, E., Tarrés, Q., Domínguez-Robles, J., Delgado-Aguilar, M., Mutjé, P., Rodríguez, A., 2018. Recycled fibers for fluting production: The role of lignocellulosic micro/nanofibers of banana leaves. J. Clean. Prod. 172, 233-238.

*FAO*. *FAOSTAT.*(2016). September.2018.

García, A., Gandini, A., Labidi, J., Belgacem, N., Bras, J., 2016. Industrial and crop wastes: A new source for nanocellulose biorefinery. Ind. Crop. Prod. 93, 26-38.

Gogoi, B. K., Oswalt, A. J., Choudhury, G. S., 1996. Reverse screw element(s) and feed Composition effects during twin-screw extrusion of rice flour and fish muscle blends. J. Food. Sci. 61(3), 590-595.

Henriksson, M., Henriksson, G., Berglund, L. A., Lindström, T., 2007. An environmentally friendly method for enzyme-assisted preparation of microfibrillated cellulose (MFC) nanofibers. Eur. Polym. J. 43(8), 3434-3441.

Ho, T. T. T., Abe, K., Zimmermann, T., Yano, H., 2015. Nanofibrillation of pulp fibers by twin-screw extrusion. Cellulose. 22(1), 421-433.

Hoeng, F., Denneulin, A., Reverdy-Bruas, N., Krosnicki, G., Bras, J., 2017. Rheology of cellulose nanofibrils/silver nanowires suspension for the production of transparent and conductive electrodes by screen printing. Appl. Surf. Sci. 394, 160-168.

Iwamoto, S., Nakagaito, A. N., Yano, H., 2007. Nano-fibrillation of pulp fibers for the processing of transparent nanocomposites. Appl. Phys A-Mater. 89(2), 461-466.

Lavoine, N., Desloges, I., Dufresne, A., Bras, J., 2012. Microfibrillated cellulose – Its barrier properties and applications in cellulosic materials: A review. Carbohyd. Polym. 90(2), 735-764.

Liang, M., Huff, H. E., Hsieh, F. H., 2002. Evaluating energy consumption and efficiency of a twin-screw extruder. J. Food. Sci. 67(5), 1803-1807.

Lin, C. S. K., Luque, R., 2014. *Renewable Resources and biorefineries*. Cambridge: Royal Society of Chemistry.

Lin, N., Dufresne, A., 2014. Nanocellulose in biomedicine: Current status and future prospect. Eur. Polym. J. 59, 302-325.

Liu, C., Li, B., Du, H., Lv, D., Zhang, Y., Yu, G., Peng, H., 2016. Properties of nanocellulose isolated from corncob residue using sulfuric acid, formic acid, oxidative and mechanical methods. Carbohyd. Polym. 151, 716-724.

Marx-Figini, M., 1987. The acid-catalyzed degradation of cellulose linters in distinct ranges of degree of polymerization. J. Appl. Polym. Sci. 33(6), 2097-2105.

Minor, J. L., 1994. Hornification - its origin and meaning. Prog. Pap. Recycl. 3, 93-95.

Mohanty, A. K., Misra, M., Drzal, L. T., 2002. Sustainable bio-composites from renewable resources: Opportunities and challenges in the green materials world. J. Polym. Environm. 10(1-2), 19-26.

Naderi, A., Lindström, T., Sundström, J., 2015. Repeated homogenization, a route for decreasing the energy consumption in the manufacturing process of carboxymethylated nanofibrillated cellulose? Cellulose. 22(2), 1147-1157.

Nechyporchuk, O., Belgacem, M. N., Bras, J., 2016. Production of cellulose nanofibrils: A review of recent advances. Ind. Crop. Prod. 93, 2-25.

Nechyporchuk, O., Pignon, F., Belgacem, M. N., 2015. Morphological properties of nanofibrillated cellulose produced using wet grinding as an ultimate fibrillation process. J. Mater. Sci. 50(2), 531-541.

OECD/FAO. (2014). Agricultural Outlook 2014-2023. OECD Publishing.

Perlatti, B., Forim, M. R., Zuin, V. G., 2014. Green chemistry, sustainable agriculture and processing systems: a Brazilian overview. Chem. Bio. Agro. 1(1), 5.

Puangsin, B., Yang, Q. L., Saito, T., Isogai, A., 2013. Comparative characterization of TEMPO-oxidized cellulose nanofibril films prepared from non-wood resources. Int. J. Biol. Macromol. 59, 208-213.

Putro, J. N., Kurniawan, A., Ismadji, S., Ju, Y.H., 2017. Nanocellulose based biosorbents for wastewater treatment: Study of isotherm, kinetic, thermodynamic and reusability. Environ. Nanotechnol. Monit. Manage. 8, 134-149.

Rol, F., Belgacem, M. N., Gandini, A., Bras, J., 2019. Recent advances in surface-modified cellulose nanofibrils. Prog. Polym. Sci. 88, 241-264.

Rol, F., Karakashov, B., Nechyporchuk, O., Terrien, M., Meyer, V., Dufresne, A., Bras, J., 2017. Pilot-Scale Twin Screw Extrusion and Chemical Pretreatment as an Energy-Efficient Method for the Production of Nanofibrillated Cellulose at High Solid Content. ACS Sustain. Chem. Eng. 5(8), 6524-6531.

Ruiz-Palomero, C., Soriano, M. L., Valcárcel, M., 2017. Nanocellulose as analyte and analytical tool: Opportunities and challenges. Trac-Trend Anal Chem. 87, 1-18.

Saito, T., Shibata, I., Isogai, A., Suguri, N., Sumikawa, N., 2005. Distribution of carboxylate groups introduced into cotton linters by the TEMPO-mediated oxidation. Carbohyd. Polym. 61(4), 414-419.

Segal, L., Creely, J. J., Martin, A. E., Conrad, C. M., 1959. An empirical method for estimating the degree of crystallintiy of native cellulose using X-ray diffractometer. Text. Res. J. 29, 786-974.

Shinoda, R., Saito, T., Okita, Y., Isogai, A., 2012. Relationship between Length and Degree of Polymerization of TEMPO-Oxidized Cellulose Nanofibrils. Biomacromolecules. 13(3), 842-849.

Spence, K. L., Venditti, R. A., Rojas, O. J., Habibi, Y., Pawlak, J.J., 2011. A comparative study of energy consumption and physical properties of microfibrillated cellulose produced by different processing methods. Cellulose. 18(4), 1097-1111.

Tarres, Q., Saguer, E., Pelach, M. A., Alcala, M., Delgado-Aguilar, M., Mutje, P., 2016. The feasibility of incorporating cellulose micro/nanofibers in papermaking processes: the relevance of enzymatic hydrolysis. Cellulose. 23(2), 1433-1445.

Tuck, C. O., Pérez, E., Horváth, I. T., Sheldon, R. A., Poliakoff, M., 2012. Valorization of Biomass: Deriving More Value from Waste. Science. 337(6095), 695-699.

Vallejos, M. E., Felissia, F. E., Area, M. C., Ehman, N. V., Tarrés, Q., Mutjé, P., 2016. Nanofibrillated cellulose (CNF) from eucalyptus sawdust as a dry strength agent of unrefined eucalyptus handsheets. Carbohyd. Polym. 139, 99-105.

Venturi, D., Grupkovic, D., Sisti, L., Baschetti, M. G., 2018. Effect of humidity and nanocellulose content on Polyvinylamine-nanocellulose hybrid membranes for $CO_2$ capture. J. Membrane. Sci. 548, 263-274.

Tao Zhang., Guojun Cai., Songyu Liu.,2018. Assessment of mechanical properties in recycled lignin-stabilized silty soil as base fill material. J. Clean. Prod. 172, 1788-1799.

**Table 1.** Characterization of the different types of lignocellulose nanofibers.

| **LCNF type** | **Nanofibrillation yield** (%) | **Transmittance** (%) | **Cationic demand** (μeq·g/g) | **Carboxyl content** (μeq·g/g) | **Specific surface area** ($m^2$/g) | **Diameter** (nm) | **Length**[*] (nm) | **Aspect ratio** |
|---|---|---|---|---|---|---|---|---|
| HPH | 55.6 ± 5.26 | 55 | 441.06 ± 7.50 | 64.41 ± 2.36 | 183.4 | 13 | 4939 | 379 |
| UFG | 35.8 ± 1.20 | 25 | 269.19 ± 38.07 | 41.05 ± 7.04 | 111.1 | 22 | 4163 | 189 |
| TSE | 15.17 ± 4.20 | 16 | 307.83 ± 9.68 | 49.35± 1.73 | 125.8 | 20 | 4437 | 221 |
| Enz–TSE | 42.31 ± 0.01 | 27 | 407.08 ± 18.57 | 65.00± 0.14 | 166.7 | 15 | 991 | 66 |

[*] Calculated as (4.286·DP) – 757 (Shinoda, Saito, Okita, and Isogai, 2012).

Table 2. Physical properties evolution of recycled cardboard substrate reinforced with different types of LCNFs and mechanical beating (PFI beating)

| Sample | | Thickness (µm) | Density (g/cm$^3$) | Porosity (%) | Gurley (s) |
|---|---|---|---|---|---|
| Recycled Cardboard | | 151.25 ± 7.21 | 0.39 ± 0.03 | 73.94 ± 1.73 | 1.60 ± 0.02 |
| PFI (rev) | 1000 | 139.25 ± 8.63 | 0.43 ± 0.03 | 71.30 ± 1.71 | 4.80 ± 0.34 |
| | 2000 | 134.33 ± 1.91 | 0.44 ± 0.02 | 70.44 ± 0.63 | 5.53 ± 0.11 |
| | 3000 | 135.83 ± 8.40 | 0.43 ± 0.02 | 70.18 ± 1.68 | 6.54 ± 0.13 |
| HPH (%) | 1.5% | 126.00 ± 9.88 | 0.46 ± 0.04 | 68.99 ± 2.96 | 7.32 ± 1.18 |
| | 3% | 120.50 ± 8.45 | 0.47 ± 0.05 | 68.58 ± 3.47 | 9.25 ± 0.34 |
| | 4.5% | 118.50 ± 9.89 | 0.49 ± 0.03 | 67.58 ± 2.44 | 18.71 ± 1.45 |
| UFG (%) | 1.5% | 133.25 ± 2.29 | 0.44 ± 0.01 | 70.62 ± 0.77 | 7.32 ± 0.18 |
| | 3% | 120.00 ± 5.41 | 0.48 ± 0.02 | 67.39 ± 1.60 | 8.64 ± 0.71 |
| | 4.5% | 120.25 ± 2.82 | 0.49 ± 0.00 | 67.50 ± 0.48 | 10.22 ± 0.13 |
| TSE (%) | 1.5% | 128.58 ± 1.13 | 0.44 ± 0.01 | 70.62 ± 1.06 | 3.72 ± 0.20 |
| | 3% | 126.17 ± 3.41 | 0.44 ± 0.01 | 71.07 ± 0.89 | 6.00 ± 0.46 |
| | 4.5% | 126.42 ± 3.90 | 0.46 ± 0.03 | 69.43 ± 2.12 | 6.91 ± 0.36 |
| TSE-Enz (%) | 1.5% | 132.17 ± 0.88 | 0.45 ± 0.00 | 69.80 ± 0.27 | 4.84 ± 0.53 |
| | 3% | 122.25 ± 3.36 | 0.46 ± 0.01 | 68.60 ± 0.72 | 5.21 ± 0.18 |
| | 4.5% | 121.00 ± 6.71 | 0.49 ± 0.03 | 67.10 ± 2.14 | 5.67 ± 0.35 |

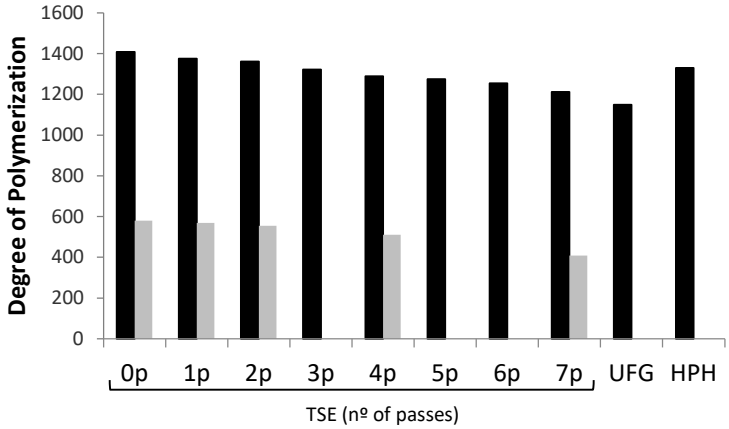


Figure 1. Variation of the degree of polymerization in the different types of LCNFs after each pass of mechanical refining. Grey and black bars correspond to nanofibers obtained with and without an enzymatic pretreatment.

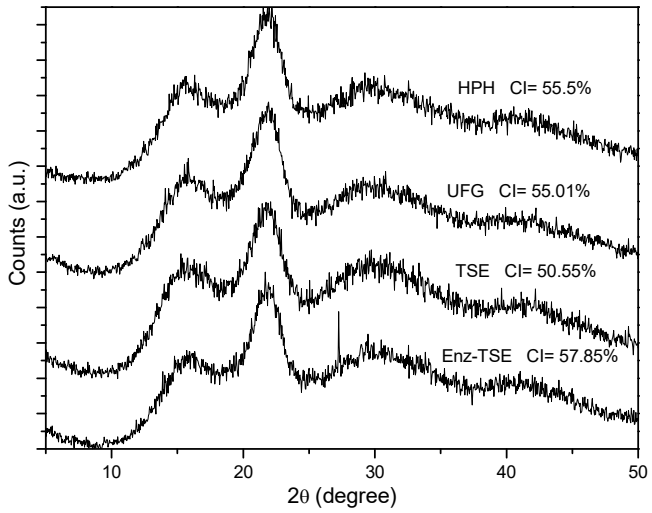


Figure 2. XRD spectra for the LCNFs.

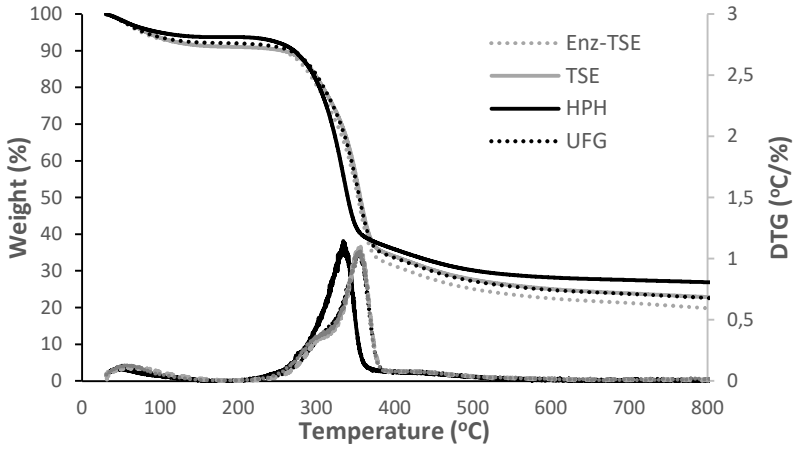


| | DTG ($T_{max}$) |
|---|---|
| **HPH** | 333 ˚C |
| **UFG** | 356 ˚C |
| **TSE** | 354 ˚C |
| **Enz-TSE** | 354 ˚C |

Figure 3. Thermogravimetric analysis of the LCNFs.

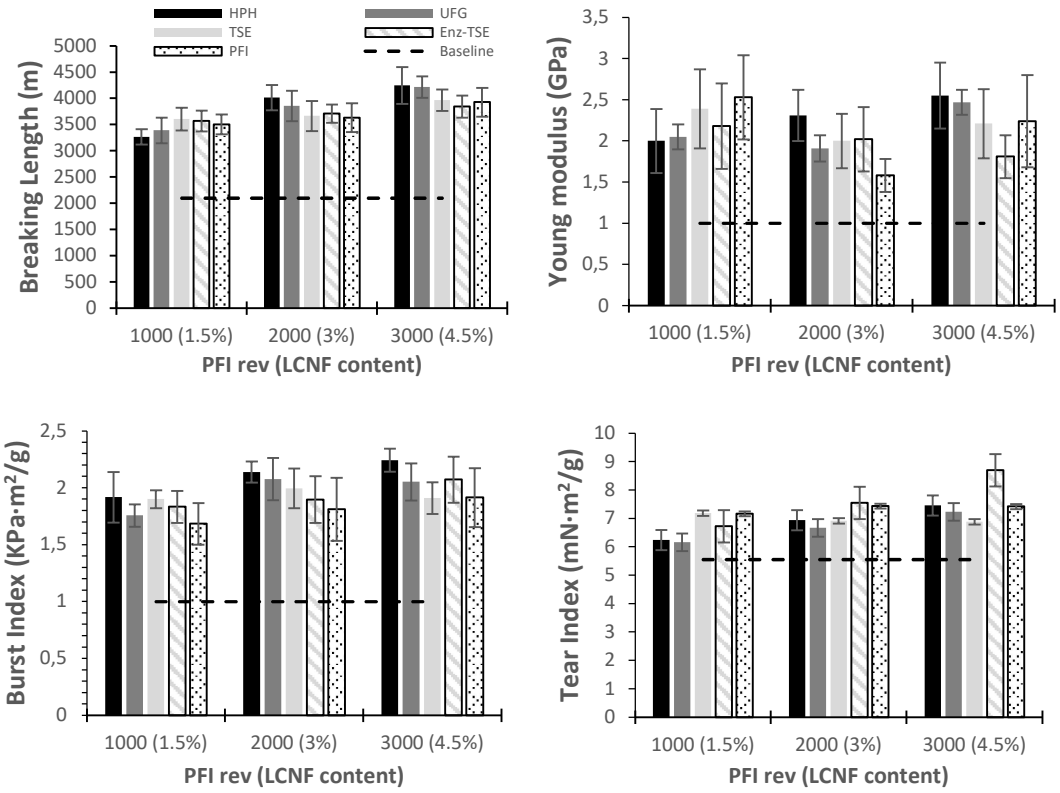


Figure 4. Reinforcing effect of the different types of LCNFs as compared with PFI refining over the recycled cardboard substrate (broken baseline).

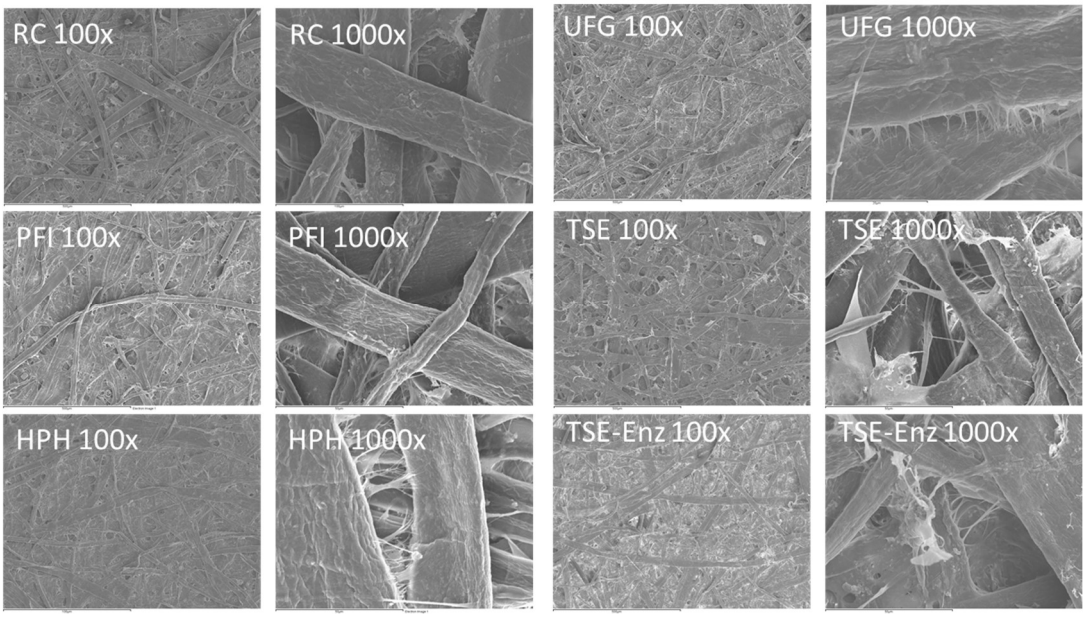


Figure 5. SEM images of recycled cardboard (RC) reinforced with LCNF (4.5%) and PFI refining (3000 rev)

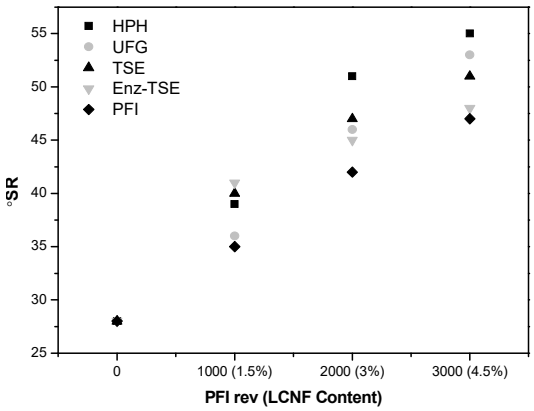


Figure 6. Variation of the drainage properties of recycled cardboard slurries upon addition of LCNFs and PFI beating.

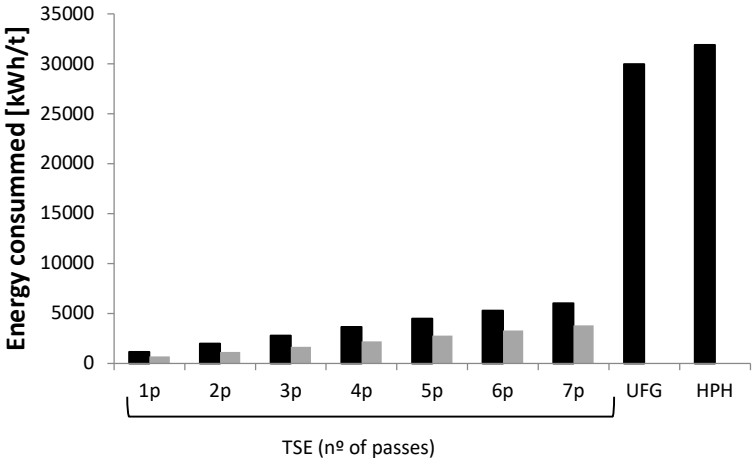


Figure 7. Energy consumption in the different treatments. Grey and black bars correspond to nanofibers obtained with and without an enzymatic pretreatment.

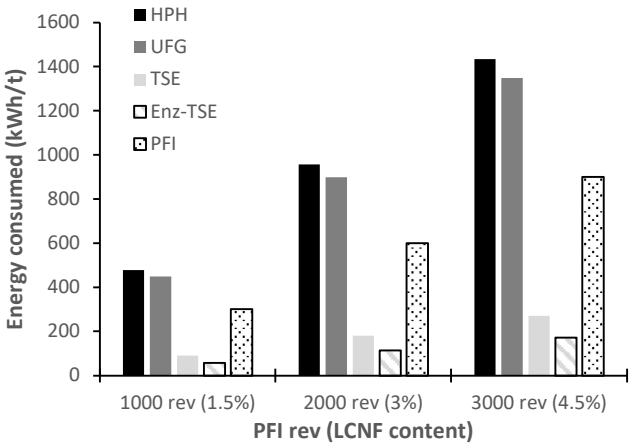


Figure 8. Energy consumption in the different mechanical treatments as compared to PFI beating.